33rd Annual International Conference of the IEEE EMBS
Boston, Massachusetts USA, August 30 - September 3, 2011

Ultrasonic Tissue Characterization of Prostate Biopsy Tissues by Ultrasound Speed Microscope

Hideki Tanoue, Yoshihiro Hagiwara, Kazuto Kobayashi, Yoshifumi Saijo, *Member, IEEE*

***Abstract*— Ultrasound speed microscope was developed for quantitative measurement of ultrasonic parameters of soft tissues. The system can measure the ultrasonic attenuation and sound speed in the tissue using fast Fourier transform of a single pulsed wave instead of burst waves used in conventional acoustic microscopy. Prostate biopsy tissues were formalin-fixed and sectioned approximately 5-6 μm in thickness. They were mounted on glass slides without cover slips. The ultrasonic transducer was mechanically scanned over the specimen. Attenuation was 1.42±0.08 dB/mm and the sound speed was 1584±12 m/s in prostatic cancer while both values were 1.86±0.14 dB/mm and 1614±30 m/s in normal prostate. The basic measurements of ultrasonic properties would help understanding the interpretation of clinical echography in diagnosis of prostate cancer.**

I. Introduction

DEFINITIVE diagnosis of prostate cancer is performed using core-needle biopsies, and the standard means of guiding core-needle biopsies of the prostate is conventional transrectal ultrasound (TRUS) imaging. Typically, the cancer tissues proven by pathologic examination were hypoechoic in echo texture. Areas of moderate echogenicity were found on pathologic examination to be secondary to ingrowth of tumor into the central area of benign hyperplastic tissue [1]. However, TRUS does not reliably distinguish between cancerous and non-cancerous tissue in the prostate; therefore, TRUS-guided biopsies simply use typically well-imaged anatomical structures, such as the interface between the gland and periprostatic fibroadipose tissues, as a spatial reference for placing core needles in the gland. Recently, new methods of tissue-type imaging that are based on spectrum analysis of echo signals and that utilize artificial neural networks for classification offer better reliably distinguishing cancerous lesions from non-cancerous tissue in the prostate than conventional echography [3].

The ultrasonic properties of various tissues and cells have been investigated by scanning acoustic microscopy (SAM) since 1980s [4-20]. SAM provides basic data for understanding clinical ultrasound images with lower frequency. Recently, ultrasound speed microscope (USM) was developed. USM uses a single pulsed wave instead of burst waves used in conventional SAM systems [12]. In the present study, ultrasonic properties of three types of prostate cancer are measured by USM and the relation between ultrasound parameters and malignancy of the tissue is discussed.

II. Methods

A. Instrumental Setup

An electric impulse was generated by a high speed switching semiconductor. The start of the electric pulse was within 400 ps from excitation, the pulse width was 2 ns, and the pulse voltage was 40 V. The electric pulse was input to a concave transducer with the copolymer of vinylidene fluoride and trifluoroethylene P(VDF-TrFE) used as the active element. The aperture diameter of the transducer was 1.2 mm, and the focal length was 1.5 mm. The center frequency was 100 MHz, the bandwidth (-6 dB) was 50-160 MHz, and the pulse repetition rate was 10 kHz. The diameter of the focal spot was estimated to be 15 μm at 100 MHz by taking into account the focal distance and sectional area of the transducer.

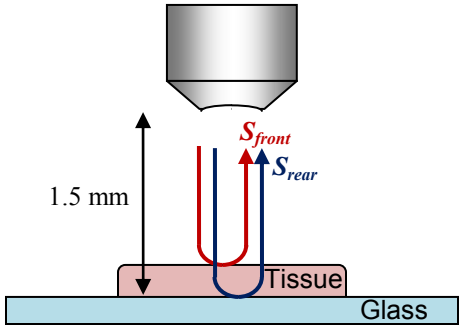

Fig. 1. Schematic illustration of the reflections at tissue and glass

Fig. 1 shows the schematic illustration of reflections. The distance from the transducer to the glass surface was 1.5 mm. Reflected wave contained two components of reflections from the surface of the tissue (S_{front}) and the interface between the

Manuscript received June 18, 2011. This project was supported in part by Grants-in-Aid for Scientific Research (Scientific Research (B) 22300175, Challenging Exploratory Research 21650125) from the Japan Society for the Promotion of Science, Sendai Advanced Preventive Health Care Services Cluster from the Ministry of Education, Culture, Sports, Science and Technology and Regional Innovation Program from the Ministry of Economy, Trade and Industry.

Hideki Tanoue is with the Graduate School of Biomedical Engineering, Tohoku University, Sendai 980-8579 Japan (e-mail: ypoons1950@nifty.com).

Yoshihiro Hagiwara is with the Graduate School of Medical Sciences, Tohoku University, Sendai 980-8575 Japan (e-mail: hagi@dent.tohoku.ac.jp).

Kazuto Kobayashi is with the Honda Electronics Co. Ltd., Toyohashi 441-3193 Japan (e-mail: kazuto@honda-el.co.jp).

Yoshifumi Saijo is with the Graduate School of Biomedical Engineering, Tohoku University, Sendai 980-8579 Japan (phone: +81-22-717-8514; fax: +81-22-795-5882; e-mail: saijo@idac.tohoku.ac.jp).

tissue and substrate (S_{rear}). The phase of the waveforms from the tissue and glass were standardized by a reflection from the glass.

Fig. 2 shows a block diagram of the USM for biological tissue characterization. A single ultrasound pulse with a pulse width of 2 ns was emitted and received by the same transducer above the specimen. Saline (0.9%) was used as the coupling medium between the transducer and the specimen. Temperature was maintained as 20 °C during whole measurements. The reflections from the tissue surface and those from the interface between the tissue and glass were received by the transducer and were introduced into a Windows-based PC with a fast digitizer card (Acqiris DP210, 2GSa/s, onboard memory 16MB, Geneva, Switzerland). The frequency range was 500 MHz, and the sampling rate was 2 GS/s. Eight consecutive values of the signal taken for a pulse response were averaged in order to reduce random noise.

The transducer was mounted on an X-Y stage driven by a XY-scan controller with a microcomputer board that was controlled by the PC through RS232C. The both X-scan and Y-scan were driven by linear servo motors and the position was detected by an encoder. The scan was controlled to reduce the effects of acceleration at the start and deceleration at the end of the X-scan. Finally, two-dimensional distributions of ultrasonic intensity, speed of sound, attenuation coefficient and thickness of a specimen measuring 2.4×2.4 mm were visualized using 300×300 pixels. The total scanning time was 63 s.

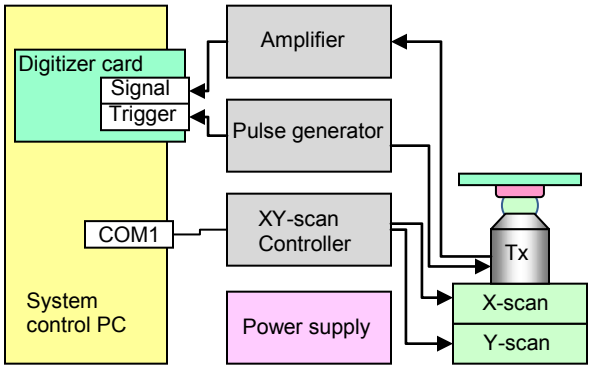

Fig. 2. Block diagram of ultrasound speed microscope (USM)

B. *Signal Analysis* [15]

Denoting the standardized phase of the reflection wave at the tissue surface as ϕ_{front}, the standardized phase at the interference between the tissue and the substrate as ϕ_{rear},

$$2\pi f \times \frac{2d}{c_o} = \phi_{front} \qquad (1)$$

$$2\pi f \times 2d\left(\frac{1}{c_o} - \frac{1}{c}\right) = \phi_{rear} \qquad (2)$$

where d is the tissue thickness, c_o is the sound speed in coupling medium and c is the sound speed in the tissue.

Thickness is obtained as

$$d = \frac{c_o}{4\pi f}\phi_{front} \qquad (3)$$

Finally, sound speed is calculated as

$$c = \left(\frac{1}{c_o} - \frac{\phi_{rear}}{4\pi fd}\right)^{-1} \qquad (4)$$

After determination of the thickness, attenuation of ultrasound at 100 MHz was then calculated by dividing amplitude by the thickness.

C. *Biopsy Prostate Tissues*

Prostate tissue was obtained by TRUS guided biopsy. All biopsy results were reviewed and assigned a Gleason score, and all surgical specimens were examined. When at least one biopsy revealed adenocarcinoma in only one lobe, the biopsy was designated as unilateral positive. Likewise, when at least one biopsy showed adenocarcinoma in each lobe, the biopsy was designated as bilateral positive.

All patients involved in this study provided written informed consent. Biopsied specimens from patients were fixed by 4% formaldehyde overnight, and embedded in paraffin by using standard processing for histology. The paraffin blocks were stored in a refrigerator at 5 °C. The samples for the acoustic microscopy were de-paraffinized without staining for acoustic microscopy. The neighboring section for USM was stained with Hematoxylin-Eosin staining for optical microscopy.

III. Results

Fig. 3 shows the optical and ultrasonic intensity images of the normal prostate tissue. Some tubular structures of the normal prostate are observed in the intensity image.

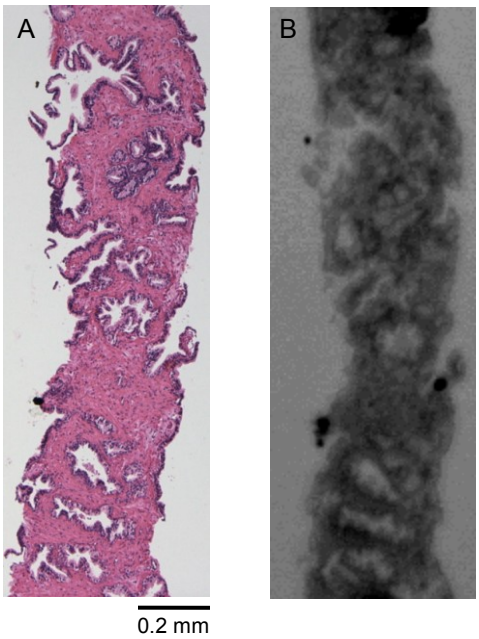

Fig. 3. Optical and ultrasound images of normal prostate.
A: Optical image (H-E staining), B: Ultrasonic intensity image

Fig. 4 shows the attenuation and sound speed images. The average value of attenuation is 1.86±0.14 dB/mm and the average value of sound speed is 1614±30 m/s.

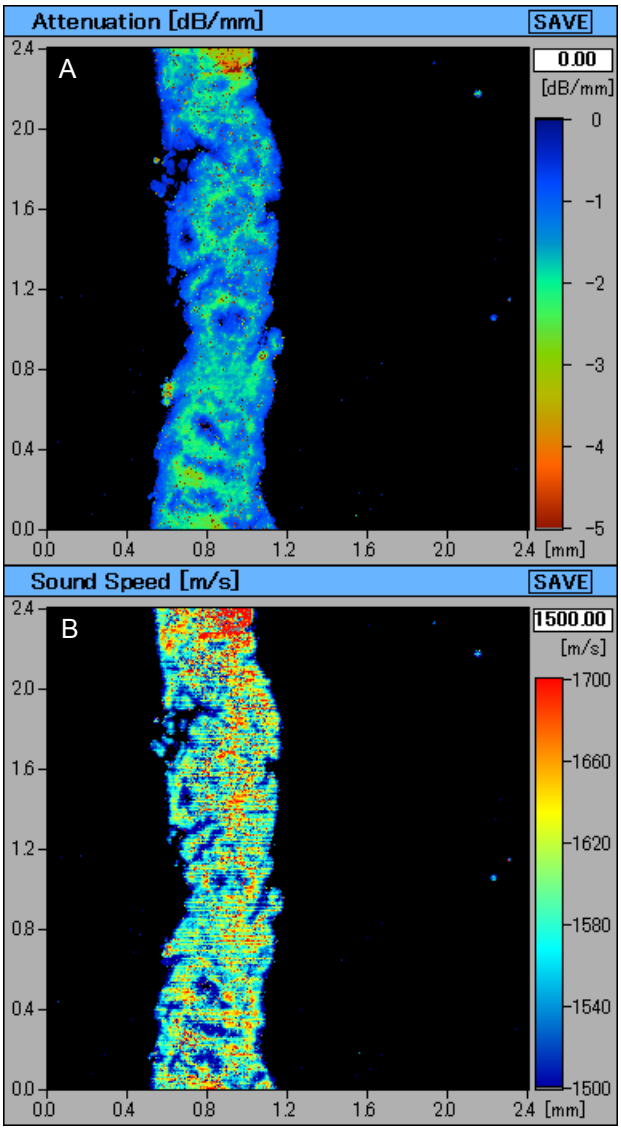

Fig. 4. Ultrasound images of normal prostate.
A: Attenuation image, B: Sound speed image

Fig. 5 shows the optical and ultrasonic intensity images of the prostatic cancer tissue. Tubular structures are destroyed and infiltration of cancer cells is observed. Fig. 6 shows the attenuation and sound speed images. The average value of attenuation is 1.42±0.08 dB/mm and the average value of sound speed is 1584±12 m/s. The attenuation is significantly lower than that of normal prostate tissue. The striated regions were excluded for calculation of average sound speed.

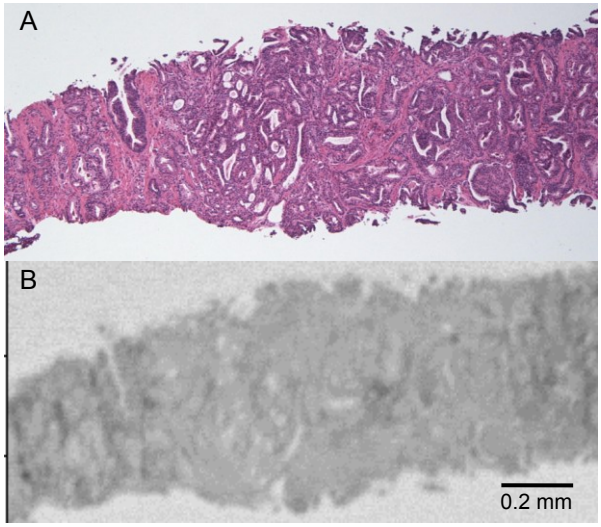

Fig. 5. Optical and ultrasound images of prostatic cancer.
A: Optical image (H-E staining), B: Ultrasonic intensity image

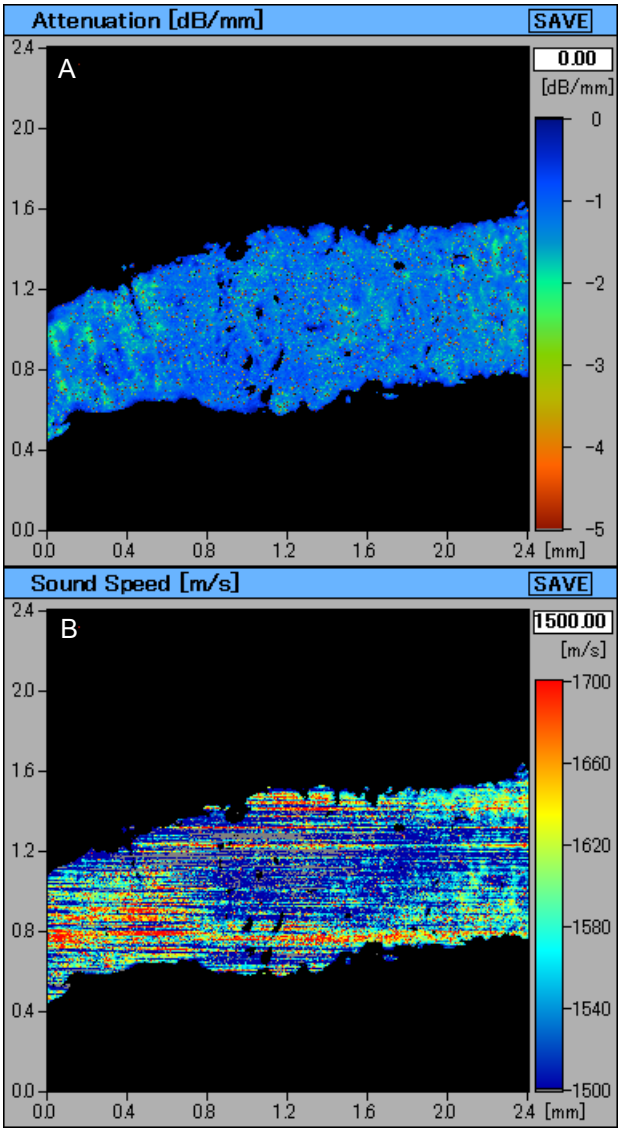

Fig. 6. Ultrasound images of prostatic cancer
A: Attenuation image, B: Sound speed image

IV. Discussion

USM has enabled the measurement of sound speed at microscopic level. Generally, density ρ and sound speed c determine the characteristic acoustic impedance Z of the material as

$$Z = \rho c$$

On the assumption that the interface between two fluid-like media (medium a and medium b) is infinite and plane, the relative reflected sound power, in dB, can be determined by the specific acoustic impedance of each medium as

$$dB = 10\log_{10}\frac{P_r}{P_i} = 10\log_{10}\frac{(Z_a - Z_b)^2}{(Z_a + Z_b)^2}$$

(P_r: sound power reflected at interface, P_i: incident sound power, Z_a: acoustic impedance of medium a, Z_b: acoustic impedance of medium b)

The density of the biological soft tissues does not differ significantly, thus the acoustic impedance is mostly determined by sound speed. Although focused ultrasound was used in the present measurement, the difference of acoustic impedance between tissues still has close correlation with echo intensity in clinical ultrasonography. The sound speed of the tubular structure was higher than the surrounding tissue. Medium or high intensity echo is expected from this "acoustic structure". On the other hand, the sound speed distribution in the prostatic cancer was homogeneous and the attenuation is lower than that of normal prostate. Hypoecho typically observed in clinically detected cancer is expected from such acoustic structure. Fibrosis in both benign and malignant tissues showed high sound speed. The collagen content in cancer may affect the echogenicity. The high echo zone at the fibrosis-adipose interface is also well explained by the difference of acoustic impedance.

V. Conclusions

Ultrasound speed microscope (USM) was equipped for ultrasonic tissue characterization of biopsy prostate tissues. The average value of attenuation is 1.86±0.14 dB/mm and the average value of sound speed is 1614±30 m/s in normal prostate. The average value of attenuation is 1.42±0.08 dB/mm and the average value of sound speed is 1584±12 m/s. in prostatic cancer. These results help understanding the intensity and texture of prostate cancer in clinical diagnosis.

References

[1] F. Lee, J.M. Gray, R.D. McLeary, T.R. Meadows, G.H. Kumasaka, G.S. Borlaza, W.H. Straub, F. Lee, Jr., M.H. Solomon, T.A. McHugh, R.M. Wolf, Transrectal ultrasound in the diagnosis of prostate cancer: Location, echogenicity, histopathology, and staging, *The Prostate*, 7 (1985), pp. 117-129.

[2] E. J. Feleppa, Ultrasonic tissue-type imaging of the prostate: Implications for biopsy and treatment guidance, *Cancer Biomarkers* 4 (2008), pp. 201-212.

[3] M. Tanaka, H. Okawai, N. Chubachi, J. Kushibiki, T. Sannomiya, Propagation properties of ultrasound in acoustic microscopy through a double-layered specimen consisting of thin biological tissue and its holder, *Jpn J Appl Phys* 23 (1984), pp. 197-199.

[4] Y. Saijo, M. Tanaka, H. Okawai, F. Dunn, The ultrasonic properties of gastric cancer tissues obtained with a scanning acoustic microscope system, *Ultrasound Med Biol* 17 (1991), pp. 709-714.

[5] A. F. van der Steen, M. H. Cuypers, J. M. Thijssen, P. C. de Wilde, Influence of histochemical preparation on acoustic parameters of liver tissue: a 5-MHz study, *Ultrasound Med Biol* 17 (1991), pp. 879-91.

[6] G. A. Briggs, J. Wang, R. Gundle, Quantitative acoustic microscopy of individual living human cells, *J Microsc* 172 (1993), pp.3-12.

[7] H. Sasaki, M. Tanaka, Y. Saijo, H. Okawai, Y. Terasawa, S. Nitta, K. Suzuki, Ultrasonic tissue characterization of renal cell carcinoma tissue, *Nephron* 74 (1996), pp. 125-130.

[8] Y. Saijo, M. Tanaka, H. Okawai, H. Sasaki, S. Nitta, F. Dunn, Ultrasonic tissue characterization of infarcted myocardium by scanning acoustic microscopy, *Ultrasound Med Biol* 23 (1997), pp. 77-85.

[9] Y. Saijo, H. Sasaki, H. Okawai, S. Nitta, M. Tanaka, Acoustic properties of atherosclerosis of human aorta obtained with high-frequency ultrasound, *Ultrasound Med Biol* 24 (1998), pp. 1061-1064.

[10] J. Bereiter-Hahn, H. Lüers, Subcellular tension fields and mechanical resistance of the lamella front related to the direction of locomotion, *Cell Biochem Biophys* 29 (1998), pp. 243-62.

[11] Y. Saijo, H. Sasaki, M. Sato, S. Nitta, M. Tanaka, Visualization of human umbilical vein endothelial cells by acoustic microscopy, *Ultrasonics* 38 (2000), pp. 396-399.

[12] S. Bumrerraj, J. L. Katz, Scanning acoustic microscopy study of human cortical and trabecular bone, *Ann Biomed Eng* 29 (2001), pp. 1034-42.

[13] Y. Saijo, T. Ohashi, H. Sasaki, M. Sato, C.S. Jorgensen, S. Nitta, Application of scanning acoustic microscopy for assessing stress distribution in atherosclerotic plaque, *Ann Biomed Eng* 29 (2001), pp. 1048-53.

[14] H. Sasaki, Y. Saijo, M. Tanaka, S. Nitta, Influence of tissue preparation on the acoustic properties of tissue sections at high frequencies, *Ultrasound Med Biol* 29 (2003), pp. 1367-72.

[15] N. Hozumi, R. Yamashita, C.K. Lee, M. Nagao, K. Kobayashi, Y. Saijo, M. Tanaka, N. Tanaka, S. Ohtsuki, Time-frequency analysis for pulse driven ultrasonic microscopy for biological tissue characterization, *Ultrasonics* 42 (2004), pp. 717-722.

[16] L. R. Taggart, R. E. Baddour, A. Giles, G. J. Czarnota, M. C. Kolios, Ultrasonic characterization of whole cells and isolated nuclei, *Ultrasound Med Biol* 33(2007), pp.389-401.

[17] Y. Saijo, N. Hozumi, K. Kobayashi, N. Okada, E. D. Santos Filho, H. Sasaki, T. Yambe, M. Tanaka, Ultrasonic tissue characterization of atherosclerosis by a speed-of-sound microscanning system, *IEEE Trans Ultrason Ferroelectr Freq Control* 54 (2007), pp. 1571-1577.

[18] E. C. Weiss, P. Anastasiadis, G. Pilarczyk, R. M. Lemor, P. V. Zinin, Mechanical properties of single cells by high-frequency time-resolved acoustic microscopy, *IEEE Trans Ultrason Ferroelectr Freq Control* 54(2007), pp. 2257-71.

[19] K. Raum, Microelastic imaging of bone, *IEEE Trans Ultrason Ferroelectr Freq Control* 55 (2008), pp. 1417-31.

[20] Y. Hagiwara, A. Ando, E. Chimoto, Y. Saijo, K. Ohmori-Matsuda, E. Itoi, Changes of articular cartilage after immobilization in a rat knee contracture model, *J Orthop Res* 27 (2009), pp. 236-242.